Photocurrent spectroscopy of deep levels in ZnO thin films

H. Frenzel,* H. v. Wenckstern, A. Weber, H. Schmidt, G. Biehne, H. Hochmuth, M. Lorenz, and M. Grundmann
Fakultät für Physik und Geowissenschaften, Institut für Experimentelle Physik II, Universität Leipzig, Linnéstrasse 5, 04103 Leipzig, Germany

(Received 9 November 2006; revised manuscript received 20 February 2007; published 31 July 2007)

Epitaxial ZnO(0001) thin films have been grown by pulsed-laser deposition on a-Al_2O_3 and investigated by deep level transient spectroscopy (DLTS) and by Fourier transform infrared photocurrent (FTIR-PC) spectroscopy in the midinfrared wavelength range. FTIR-PC spectra of undoped ZnO layers show several well-resolved spectral features between 100 and 500 meV due to transitions from deep defect states either to the conduction band or to the valence band. They include the commonly observed intrinsic deep defects E1 at ~110 meV and E3 at ~320 meV. DLTS and FTIR-PC measurements were repeated after annealing the samples either in vacuum, under oxygen, or nitrogen atmospheres. Based on annealing effects, the possible microscopic origin of major deep levels in the ZnO samples is discussed. Further FTIR-PC investigations of Co- and Mn-doped ZnO reveal defect levels at ~270, ~380, and ~450 meV and are compared with corresponding DLTS data.

DOI: 10.1103/PhysRevB.76.035214 PACS number(s): 71.55.Gs, 73.30.+y

I. INTRODUCTION

ZnO is a suitable material for applications in ultraviolet (UV) optoelectronics due to its wide band gap and large exciton binding energy. It is a candidate for UV lasers, blue, green, orange, and UV light-emitting diodes[1] as well as for transparent electronics and displays.[2] Below the Curie temperature (predicted to lie above room temperature for ZnO), ZnO doped with 3d transition metal (TM) ions combines the charge and spin degrees of freedom for potential use in future spintronic devices.[3] Most importantly, the state of magnetization changes the electronic properties and vice versa through the spin exchange interaction between the local magnetic moments and carriers.[4]

One important step to realize diodes or spintronic devices is the control of the conductivity. Nominally undoped ZnO is usually n-type conducting due to intrinsic donorlike defects.[5] A pn junction is recommended for the injection of both charge carrier types. Until now, there are still difficulties in producing p-type conducting ZnO. Thus, it is important to investigate and control the formation of electron and hole traps in ZnO.

By means of photocurrent and Fourier transform infrared photocurrent (FTIR-PC) measurements, so far only effective-mass impurities and mostly hydrogen-related defects with a thermal activation energy less than 100 meV were studied.[6,7] Deep donor levels in ZnO have mostly been investigated by deep level transient spectroscopy (DLTS). In order to identify defects, their formation is affected by the thin film growth and sample annealing conditions. Cordaro and Shim[8] found levels at ~170 and ~330 meV below the conduction band edges, labeled T1 and T2, respectively, and related them to the second ionization of zinc interstitial and the oxygen vacancy. Other groups reported L1 (close to T1) and L2 at ~170 and ~260 meV,[9] and E1, E3 (close to T2), and E4 at ~120, ~290, and ~570 meV, respectively.[10] Due to the lack of accurate theoretical predictions, the identification of the microscopic origin of experimentally detected electronic defects remains an open issue.

With DLTS, only rechargeable defects with a sufficiently large thermal capture cross section are observable. FTIR-PC spectroscopy as an optical method has a better energy resolution than DLTS by probing optical transitions either into a band or into shallow states below the band edge. However, FTIR-PC is not capable to distinguish between minority and majority traps, which makes the interpretation ambiguous in some cases.

In Sec. III, we investigate influences of annealing conditions and doping on the formation of deep intrinsic defects in ZnO. The combination of the complementary methods FTIR-PC and DLTS enables us to study both optical and thermal carrier excitations. FTIR-PC and DLTS are generally comparable, assuming that the thermal activation energy is similar to the optical ionization energy. However, depending on electric-field assisted emission or lattice relaxation, the thermal activation energies determined by DLTS are expected to be smaller than the transition energies from FTIR-PC.

II. SAMPLE PREPARATION AND EXPERIMENTAL SETUP

Three series (A, B, and C), each consisting of four samples, were investigated. Series A serves as reference for the study of annealing and target influences in series B. Both series are nominally undoped. The samples of series C were doped with Mn or Co.

The (0001)-oriented ZnO thin films were grown by pulsed-laser deposition (PLD) on a-plane sapphire substrates at a temperature of about 700 °C. The ceramic PLD targets have been prepared using a standard powder chemical route by mixing and pressing appropriate amounts of oxide powders. A degenerate ZnO:Al layer ($d \sim 50$ nm) was first deposited on the Al_2O_3 substrate and contacted from the sides by sputtered Au. This layer serves as Ohmic back contact assuring very low series resistances (typically 50–200 Ω).[11] The ZnO layer is about 1 μm thick and either nominally undoped (series A and B) or doped with an amount of 0.2% and 2% Mn or Co (series C). High-quality Pd-ZnO-Schottky diodes were realized by thermal evaporation of 10 nm Pd without additional previous cleaning procedures.

 ©2007 The American Physical Society

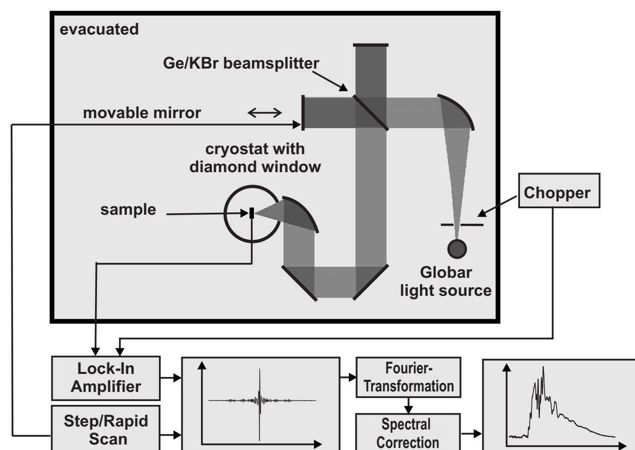

FIG. 1. Experimental setup of FTIR-PC.

Series A consists of *four individually* grown samples with nominally equal growth conditions as series B. For series B, we divided *one* sample into four parts. Thus, with regard to initial conditions, series B is more reliable in the further discussions. One sample of series A (B) was left in the as-grown state while the other three samples (parts) were annealed for 1 h at 700 °C either in vacuum, under oxygen, or nitrogen atmosphere (800 mbar), respectively. With this treatment, the formation of several deep intrinsic defects such as zinc interstitials or oxygen vacancies into the ZnO lattice can be studied. A further difference between series A and B is the pretreatment of the ZnO target in the PLD process. In the case of series A, it was presputtered by several thousand laser pulses while for series B, the target was not presputtered.

Figure 1 shows a scheme of the experimental setup used for FTIR-PC measurements on Schottky diodes. The spectra were recorded using a Bruker IFS 66v/S Fourier spectrometer, which has been evacuated to prevent absorption from air. The Planck spectrum of a globar ($T \sim 720$ K) serves as an infrared light source. The emitted light ($\lambda \sim 3-50$ μm) enters through a variable aperture into the Michelson interferometer and is then focused onto the sample. The sample serves as the detector by generating a photocurrent in response to optical transitions in the region near the valence band and conduction band. It is mounted in a liquid-helium cryostat equipped with a diamond window and cooled to a temperature of 4.2 K. A lock-in amplifier setup is used to filter the signal from the electric noise and thermal background. In order to compare respective FTIR-PC spectra, they were spectrally corrected with a calibrated reference spectrum. However, the responsivity is also dependent on the characteristics of the Schottky barrier diode. Therefore, an offset can occur in the FTIR-PC spectra. Further, the geometric contact area is not equal to the optically sensitive contact area due to different shadowing from silver contacts. For evaluation of FTIR-PC spectra, only the use of relative peak heights is appropriate. DLTS data were taken between 20 and 330 K using a PhysTech FT 1030 DLTS measurement system. The lock-in frequency was varied between 1 and 1000 Hz. The diodes were reversely biased with −3 V. A filling pulse height of 3 V (−3–0 V) and filling pulse lengths ranging from 1 to 100 ms were used.

III. RESULTS

Current-voltage measurements of series A and B show a rectifying behavior. For samples treated in vacuum or oxygen, this property degrades. In contrast, annealing in nitrogen improves the rectification property, probably due to a change of the surface Fermi level. Such diodes exhibit ideality factors below 1.5 and low leakage current densities (10^{-3} A cm^{-2} at −1 V). Ideality factors of Co- and Mn-doped samples lie in the range between 2 and 4, which is due to additional parallel current paths and nonradiative band-impurity recombination. Calculations from capacitance-voltage measurements ($f \sim 1$ MHz) show an increase of the net doping density in all cases during annealing. This is probably caused by diffusion of Al from the ZnO:Al layer and the Al_2O_3 substrates. The free carrier concentrations of all samples lie in the range between 10^{16} cm^{-3} for the as-grown samples and 10^{17} cm^{-3} for the thermally treated samples.

A. Properties of nominally undoped ZnO films

Figures 2(a) and 2(c) depict FTIR-PC and DLTS spectra of series A. The comparison of data obtained by both methods reveals that the observed levels lie at the same energy and equal the commonly observed defects E1 at ~110 meV, E3 at ~320 meV, and L2 at ~260 meV in ZnO. This leads to the assumption that E1, E3, and L2 reveal small tunneling and Stokes shift effects only. Additionally, FTIR-PC shows a defect, labeled A2, at ~160 meV, which is usually not visible in DLTS spectra of thin ZnO films. Thus, it is most likely a hole trap,[12,13] because in *n*-type ZnO only electron transients are observable by conventional DLTS. The peak height depends on the product of respective thermal (DLTS) and optical (FTIR-PC) capture cross section and density. Assuming equal densities, A2 and L2 seem to have larger optical capture cross sections than E1 and E3 and are therefore dominant in FTIR-PC. On the other hand, E1 and E3 are predominant in DLTS due to their large thermal capture cross sections. The FTIR-PC spectra exhibit a fine structure on the larger peaks and bands. This could be on the one hand due to superpositions of defect peaks lying at similar energies. On the other hand, this could be due to optical or thermal assisted tunneling, which leads to slightly different transition energies.

Spectra of series A are only slightly depending on the annealing conditions most probably due to different initial conditions. After annealing in O_2, the peak of A2 is larger relative to L2 and E3, which could be a first hint for a connection with oxygen. DLTS spectra of the defect E3 imply that E3 is a multiple defect. As a matter of fact, in the case of the O_2 annealed sample of series A and B, the double peak structure (labeled E3/E3′) becomes clearly visible. Their corresponding thermal activation energies lie approximately between 320 and 370 meV. FTIR-PC spectra show peaks near both energies. Furthermore, the capture cross section of

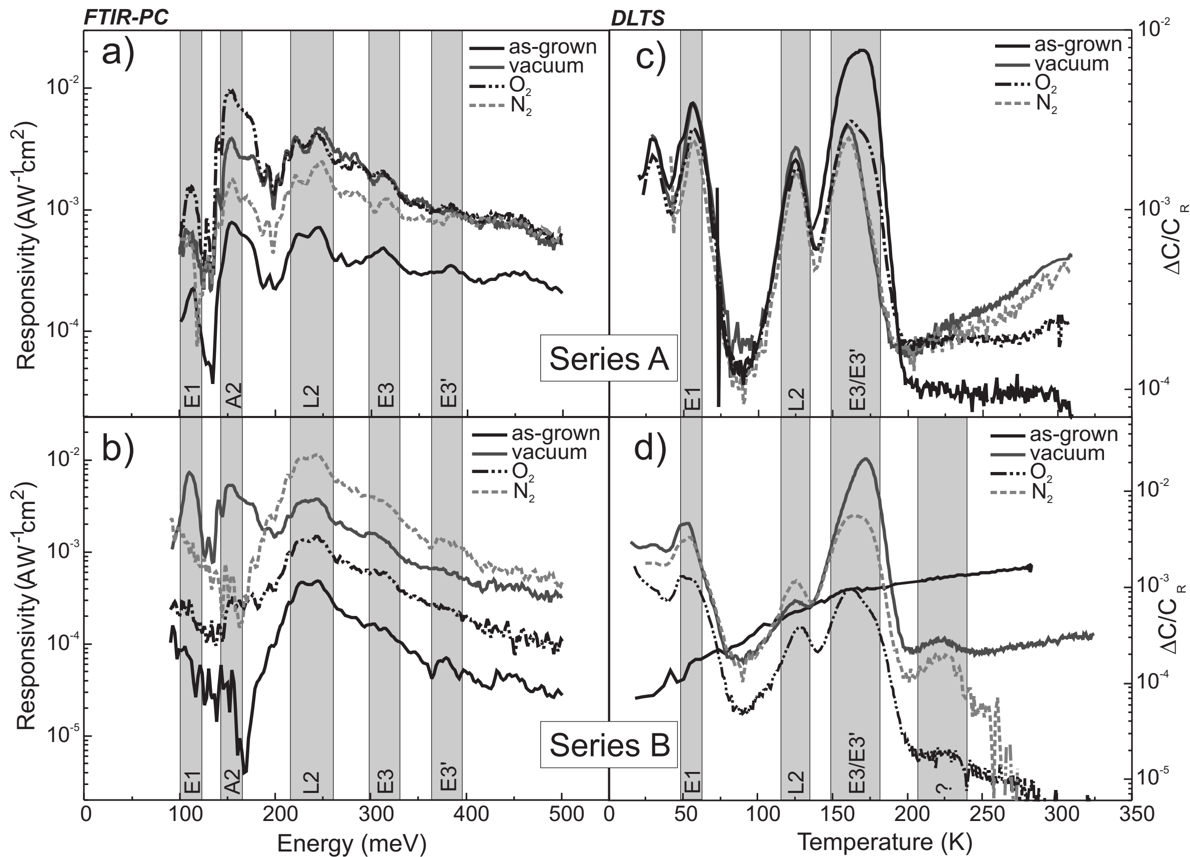

FIG. 2. [(a) and (b)] FTIR-PC spectra of differently annealed ZnO thin films. [(c) and (d)] DLTS measurements using a filling pulse of 10 ms and a lock-in frequency of 2 Hz. The gray boxes show the defect levels detected by FTIR-PC and DLTS, respectively.

E3 and E3′ must be different. This is evident from the comparison of DLTS signals recorded with different lock-in frequencies (not shown here). The defect concentrations vary between 10^{14} and 10^{16} cm^{-3} and depend strongly on the annealing conditions. It can be seen from Fig. 2(d) that E3′ dominates the spectrum of the vacuum annealed sample, whereas its intensity equals E3 in the nitrogen annealed sample. After oxygen annealing, the intensity of E3′ is the lowest. Therefore, we connect E3′ with the oxygen sublattice. The intensity of E3 after oxygen annealing did not change with respect to the as-grown state. From this significantly different response on annealing atmospheres, we assume E3 and E3′ to be not lying on the same sublattice. Thus, we follow the attribution of Brauer *et al.*[14] connecting E3 with the second ionization of zinc interstitial. Nevertheless, both possible identifications for E3 (Zn_i, V_O) are still subjects of discussions in the literature. Our recent results might explain the ongoing controversy about the identification of the E3 defect. We have proven that two closely lying levels exist in the energy range where E3 is expected and these defects show different annealing behaviors. Annealing experiments under zinc rich conditions could give further insight.

The DLTS and FTIR-PC spectra of the as-grown samples of series A and B in Fig. 2 differ largely. The as-grown sample of series B exhibits a featureless DLTS signal which cannot be analyzed by conventional maximum evaluation. The FTIR-PC spectrum is not typical as well. It does not show the existence of E1 or A2. L2 is visible as a peak, while E3 is visible as a shoulder with weak intensity only. The differences of series B and A are due to the different states of the target for the PLD growth of series B. The nonsputtering of the target before the PLD growth involves a heavily disturbed defect distribution in the ZnO layer of series B, whereas the presputtering results in a commonly known defect distribution in series A.[15] Thus, it is recommended to presputter the target before use in order to avoid the detected anomalies.

Using thermal treatments, typical defects in ZnO films are recovered in series B. Here, the comparison of defect concentration after the different anneals is unambiguous (especially if compared to series A) since all diodes of series B were produced from a single sample. DLTS spectra reveal the peaks E1, L2, and E3/E3′ for all annealing conditions. In FTIR-PC, this occurs only partially. After oxygen annealing, first hints of A2 are noticeable. A2 is obviously reactive on oxygen annealing, as it is also evident from series A. However, after annealing in vacuum, the FTIR-PC spectrum, as seen in Fig. 2(a), is restored. In the vacuum-treated sample, the concentration of E1 is at maximum. This is also evident from the dominance of the E1 peak in DLTS. However, E1 has been detected by DLTS for all treated samples but not by FTIR-PC. The concentration of E1 and E3′ is lowest for the oxygen annealed sample, which allows the

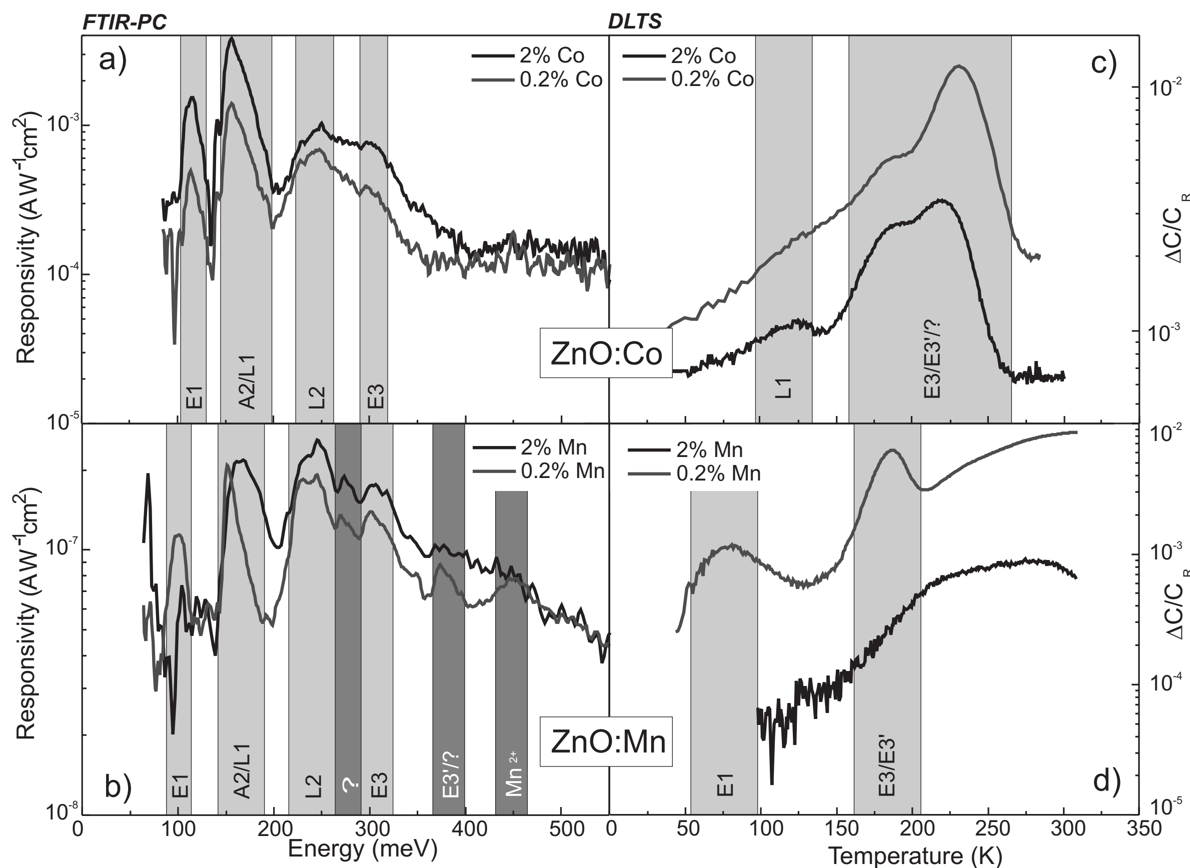

FIG. 3. [(a) and (b)] FTIR-PC spectra of Co- and Mn-doped ZnO. [(c) and (d)] DLTS measurements (Ref. 20) using a filling pulse of 1 ms and a lock-in frequency of 100 Hz. The gray boxes show the defect levels detected by FTIR-PC and DLTS, respectively.

conclusion that E1 and E3′ are related to the oxygen sublattice.

Nitrogen annealing served as reference for oxygen annealing in series A and B. Both treatments lead to similar results. However, there are differences in the behavior of E3 and E3′ (see shoulder in DLTS spectra of series A and B) and A2, which reappears after oxygen annealing of series B in FTIR-PC. One further peak that is strongest in the DLTS spectrum of the nitrogen annealed sample of series B at 225 K has an activation energy of ~400 meV. It is also visible in the corresponding FTIR-PC spectrum as a shoulder of the E3′ peak. This peak may be related to the 235 K peak of the 0.2%-Co-doped sample [see Fig. 3(c)], because it has a similar activation energy and capture cross section. This would imply that it is an intrinsic defect, increased by the Co doping, since it can be excluded that any amount of Co is present in the growth chamber of series B. However, this defect has not been detected in the FTIR-PC spectrum of the 0.2%-Co-doped sample.

Due to the width of L2 in the FTIR-PC spectra, an extended defect structure is more probable than a single point defect and confirms the statements of Freer and Leach[16] and Rohatgi *et al.*[9] that L2 cannot be a simple point defect. This would explain why L2 has mostly been detected in polycrystalline ZnO (Ref. 17) and in PLD-grown films but not in single crystals.

B. Properties of TM-doped ZnO films

Kittilstved *et al.*[18] recently described the electronic structure of Co^{2+} and Mn^{2+} ions built in ZnO. Thus, Co forms a donorlike and Mn an acceptorlike level:

$$Co^{+} \leftrightarrow Co^{2+} + e^{-}, \qquad (1)$$

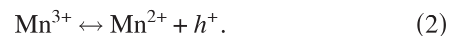

$$Mn^{3+} \leftrightarrow Mn^{2+} + h^{+}. \qquad (2)$$

Additionally, they investigated the excited states of Co and Mn within the band gap using absorption, photocurrent, and cathodoluminescence spectroscopy.[18] For Co, the transition energies amount to $E_C - E_D = 322$ meV and 1.66 eV and for Mn, the transition energies amount to $E_A - E_V = 421$ meV and −2.68 eV. The smaller energies are detectable by FTIR-PC and DLTS. X-ray photoelectron spectroscopy and electron paramagnetic resonance spectroscopy reveal that Mn is incorporated in the 2+ valence state in ZnO films for similar growth conditions as the investigated samples.[19]

Diaconu *et al.*[20] investigated electric and magnetic properties of series C. Figure 3 compares FTIR-PC and DLTS spectra of the Co- and Mn-doped ZnO films. In the FTIR-PC spectra, again the four typical defects for ZnO are visible: E1, A2, L2, and E3. In the ZnO:Co samples, E1 and A2 are predominant, while L2 and E3 are superimposed by a broad

band between 220 and 350 meV. The expected transition at 322 meV cannot be separated from E3. E3 dominates the DLTS spectra. It is shifted for the smaller concentration of Co to higher temperatures. For 2% ZnO:Co, activation energies of E3 at ~300 and a deeper defect at ~330 meV were determined. For 0.2% ZnO:Co, those energies lie at ~340 and ~390 meV. Remarkable is the appearance of the electron trap peak L1 at 120 K (~170 meV) in the DLTS spectrum of the 2% ZnO:Co sample [Fig. 3(c)]. The corresponding peak in FTIR-PC [Fig. 3(a)] is disproportionately high and its line shape is different compared to the undoped ZnO samples in Fig. 2(a). Here, the peak of the hole trap A2 is superimposed by the one of the electron trap L1. Because Co is incorporated in ZnO on the Zn position,[21] the formation of Zn_i is enhanced and one can assume that L1 is related to defects in the Zn sublattice. This was already assumed by Cordaro and Shim[8] and calculated by Han *et al.*[22] with a modified model after Sukker and Tuller.[23] However, it is most likely not a zinc interstitial, because there are only two possible transitions as double donor. The first ionization is at approximately 12–20 meV and the second ionization at ~300 meV (E3).[14] The results of Sec. III A support that. Furthermore, Mn also occupies the Zn position. The line shape of L1 in the FTIR-PC spectrum of 0.2% ZnO:Mn [Fig. 3(b)] is similar to that of ZnO:Co [Fig. 3(a)]. However, in DLTS, L1 has not been observed in ZnO:Mn. However, the quality of the ZnO:Mn samples is different. The FTIR-PC spectrum of the 2% Mn sample is noisier than that of the 0.2% sample. Responsivity of both samples is more than 2 orders of magnitude smaller than that of the Co-doped samples.

Besides the common transitions, there are two additional peaks in the 0.2% ZnO:Mn sample at ~270 and ~450 meV. They are marked with dark gray boxes in Fig. 3(b). The latter peak is close to the energy of 421 meV of the acceptorlike transition of Mn^{2+} [Eq. (2)]. A slight indication of this peak is also visible in the as-grown sample of series A. Maybe, this is also a superposition of peaks of an electron with a hole trap. The DLTS spectra only show a broad signal at higher temperatures besides E1 and E3, whereas FTIR-PC is able to resolve individual peaks in the broad band of Fig. 3(b). The peak at ~270 meV close to L2 is evident in the FTIR-PC spectra of both Mn-doped samples. Further, the peak corresponding to E3′ is larger than in series A or B. The presence of transition metal ions obviously influences the chemical environment of intrinsic defects in ZnO.

IV. SUMMARY

Investigations of PLD-grown ZnO films by DLTS and FTIR-PC show that FTIR-PC in combination with DLTS provides additional information about deep intrinsic defects. FTIR-PC probes all commonly known defects such as E1, E3, L1, and L2 with activation energies similar to the thermal activation energies determined by DLTS. It can be seen that FTIR-PC also probes hole traps such as A2, which may be superimposed by peaks from electron traps at the same ionization energy. This is the case in one sample doped with 2% Co, where L1 has been detected by FTIR-PC and DLTS and was superimposed by the peak of A2. In order to identify the microscopic nature of those defects, samples have been grown under equal growth conditions and annealed in different ambient gases. It becomes apparent that presputtering the target is important before the PLD growth. DLTS suggests that E3 consists of two closely spaced levels (E3 and E3′). By studying the behavior of the peaks after thermal treatment, a relation of E3 to the zinc interstitial is more probable than a relation to the oxygen vacancy. The observed lower concentrations of E1 and E3′ in samples treated in oxygen imply a link to the oxygen sublattice. The significantly different annealing response of E3 and E3′ might explain the controverse discussions in the literature about the identification of E3.

Doping with transition metal ions influences the formation of intrinsic defects and introduces additional defects. In ZnO:Co, this leads to the formation of L1. Conclusions of this work and literature are contrary to the statement that L1 could probably be the zinc interstitial. Mn-doped ZnO shows three additional features at ~270, ~380, and ~450 meV. The fact these transitions are only observed by FTIR-PC is most probably because they do not involve the conduction band. The peak at 450 meV is due to the acceptorlike Mn^{2+} transition. At 380 and 450 meV, again a superposition of peaks from electron and hole traps is possible.

ACKNOWLEDGMENTS

This work has been supported by Deutsche Forschungsgemeinschaft in the framework of SPP1136 (Gr 1011/10-3) and BMBF (FKZ 03N8708).

*hfrenzel@physik.uni-leipzig.de

[1] S. J. Jiao *et al.*, Appl. Phys. Lett. **88**, 031911 (2006).
[2] J. F. Wagner, Science **300**, 1245 (2003).
[3] C. Liu, F. Yun, and H. Morkoç, J. Mater. Sci.: Mater. Electron. **16**, 555 (2005).
[4] Q. Xu, L. Hartmann, H. Schmidt, H. Hochmuth, M. Lorenz, R. Schmidt-Grund, C. Sturm, D. Spemann, and M. Grundmann, Phys. Rev. B **73**, 205342 (2006).
[5] S. B. Zhang, S. H. Wei, and A. Zunger, Phys. Rev. B **63**, 075205 (2001).
[6] U. Röder, D. Klarer, R. Sauer, and K. Thonke, Proceedings of the 27th International Conference on the Physics of Semiconductors, (Flagstaff, AZ, 2004), AIP Conf. Proc., 772, p. 179 (2005).
[7] E. V. Lavrov, F. Borrnert, and J. Weber, Phys. Rev. B **72**, 085212 (2005).
[8] J. F. Cordaro and Y. Shim, J. Appl. Phys. **60**, 4186 (1986).

[9] A. Rohatgi, S. K. Pang, T. K. Gupta, and W. D. Straub, J. Appl. Phys. **63**, 5375 (1988).
[10] F. D. Auret, S. A. Goodman, M. Hayes, M. J. Legodi, H. A. van Laarhoven, and D. C. Look, Appl. Phys. Lett. **79**, 3074 (2001).
[11] H. v. Wenckstern, G. Biehne, R. A. Rahman, H. Hochmuth, M. Lorenz, and M. Grundmann, Appl. Phys. Lett. **88**, 092102 (2006).
[12] A. Y. Polyakov *et al.*, J. Appl. Phys. **94**, 2895 (2003).
[13] H. v. Wenckstern, R. Pickenhain, H. Schmidt, M. Brandt, G. Biehne, M. Lorenz, and M. Grundmann, Appl. Phys. Lett. **89**, 092122 (2006).
[14] G. Brauer *et al.*, Phys. Rev. B **74**, 045208 (2006).
[15] H. Frenzel, H. v. Wenckstern, A. Weber, G. Biehne, H. Hochmuth, M. Lorenz, and M. Grundmann, Proceedings of the 28th International Conference on the Physics of Semiconductors, (Wien, Austria, 24–28 July 2006), edited by W. Jantsch and F. Schäffler, AIP Conf. Proc., 893, 301 (2007).
[16] R. Freer and C. Leach, Solid State Ionics **173**, 41 (2004).
[17] N. Shohata, T. Matsumura, and T. Ohno, Jpn. J. Appl. Phys. **19**, 1793 (1980).
[18] K. R. Kittilstved, W. K. Liu, and D. R. Gamelin, Nat. Mater. **5**, 291 (2006).
[19] M. Diaconu *et al.*, Phys. Rev. B **72**, 085214 (2005).
[20] M. Diaconu, H. Schmidt, H. Hochmuth, M. Lorenz, H. v. Wenckstern, G. Biehne, D. Spemann, and M. Grundmann, Solid State Commun. **137**, 417 (2006).
[21] M. Kobayashi, Y. Ishida, J. I. Hwang, T. Mizokawa, A. Fujimori, K. Mamiya, J. Okamoto, Y. Takeda, T. Okane, Y. Saitoh, Y. Muramatsu, A. Tanaka, H. Saeki, H. Tabata, and T. Kawai, Phys. Rev. B **72**, 201201(R) (2005).
[22] J. Han, P. Q. Mantas, and A. M. R. Senos, J. Eur. Ceram. Soc. **22**, 49 (2002).
[23] M. H. Sukker and H. L. Tuller, Adv. Ceram. **7**, 71 (1983).